PHYSICAL REVIEW B, VOLUME 63, 125108

# Optical properties of semiconductors using projector-augmented waves

B. Adolph,* J. Furthmüller, and F. Bechstedt
*Institut für Festkörpertheorie und Theoretische Optik, Friedrich-Schiller-Universität, D-07743 Jena, Germany*

(Received 20 September 2000; published 12 March 2001)

The frozen-core projector-augmented wave (PAW) method is applied to construct all-electron valence wave functions from non-norm-conserving pseudo wave functions and atomic functions. The use of all-electron wave functions possesses the advantage that no nonlocal contributions to the optical transition operator have to be taken into account. In addition, the more accurate description of the wave functions in the core region improves the quality of the calculated spectra compared to those obtained from a pseudopotential approach. We demonstrate the accuracy of the PAW approach by comparing optical spectra of several semiconductors with those obtained employing a full all-electron method or norm-conserving pseudopotentials.

DOI: 10.1103/PhysRevB.63.125108 PACS number(s): 71.15.Ap, 78.20.Bh

## I. INTRODUCTION

Recent progress in computational methods makes it possible to calculate optical spectra of semiconductors from first principles. Very recently, such first-principles calculations have even been performed including simultaneously quasiparticle effects and electron-hole interaction.[1–5] Despite the inclusion of many-body interactions, the starting point of all these calculations is a single-particle electronic structure based on density-functional theory (DFT) in the local-density approximation[6,7] (LDA) and *ab initio* norm-conserving pseudopotentials.[8]

The description of the electron-ion interaction by means of pseudopotentials (PP's) has the advantage of reducing the all-electron (AE) problem to the treatment of a few valence electrons. The core electrons, which usually do not play a role in the optical properties for not too large photon energies, can be frozen into the cores of the atoms. The disadvantage of using PP's in the calculation of optical properties is the spatial nonlocality of these potentials. Within the Coulomb gauge of the electromagnetic field the optical transition operator is related to the velocity operator $\mathbf{v}$ of the electrons. It may be related to the momentum operator $\mathbf{p}$ by $\mathbf{v}=(1/m)\mathbf{p}+(i/\hbar)[V_{nl},\mathbf{x}]$. However, an extra term appears, proportional to the commutator of the space coordinate $\mathbf{x}$ and the nonlocal contribution $V_{nl}$ to the single-particle potential.[9,10] Typical sources of such nonlocal contributions are nonlocal PP's,[10–13] or (screened) exchange interactions.[14]

Another problem in the calculation of optical transition matrix elements is the inadequate description of the core region due to the use of pseudowave functions.[13] This problem becomes even more complicated when lifting the norm-conservation condition and using non-norm-conserving ultrasoft (US) PP's of the Vanderbilt type.[15,16] On the other hand, US PP's allow the treatment of several hundreds of atoms in a unit cell, in particular for first-row elements.[17] However, the crucial step is to augment the pseudo wave functions used in the core region in a physically reasonable way. As a possible approach the inclusion of a core-repair term employing a reconstruction of AE valence wave functions within the US PP approach has been proposed in a recent paper.[13] A more consistent approach using AE valence wave functions from the very beginning is the projector-augmented wave (PAW) method.[18] Recently, a formal relationship has been demonstrated between the Vanderbilt-type US PP and the frozen-core PAW method.[19] The frozen-core PAW method turns out to be as powerful as the US PP method since it is also restricted to a variational treatment of the valence states only. The basic variational quantities are again non-norm-conserving pseudo wave functions. The major difference between the PAW and US PP methods concerns only the augmentation of the charges or wave functions inside the core region.

In the present paper we demonstrate the accuracy of the PAW approach for the calculation of optical spectra. Explicitly, we select a set of six semiconductors (diamond, Si, cubic SiC, AlP, GaAs, and InSb) with widely different bonding properties. The PAW results are compared with those obtained using a full AE method and a norm-conserving PP approach.

## II. METHODS

Within the PP approach the calculation of optical transition matrix elements, at least in the commonly used Coulomb gauge of the electromagnetic field, is accompanied by two difficulties and, hence, sources of errors. (i) Instead of the local momentum operator, the nonlocal velocity operator has to be used. (ii) The pseudo wave functions are smoother around the atomic cores in order to minimize the number of basis functions, while the actual wave functions possess nodes in the core region. The use of AE wave functions has the advantage that they are formally derived from a local AE potential. Therefore, the velocity operator used in the transverse gauge can be expressed by the momentum operator only. This is a significant simplification compared to the PP method. Augmentation of pseudo wave functions by AE wave functions as a tool for simplifying the calculation of the optical matrix elements and for fixing the errors introduced inside the pseudocore region due to the improper nodal structure of the pseudo wave functions was already suggested by Kageshima and Shiraishi.[13] In our approach we go a further step beyond by starting from a proper (frozen-core) AE approach from the very beginning. This has the advantage that all ground state properties are treated on the same consistent footing, not only a certain special aspect.

The starting point is an implementation of the PAW method[18] in an existing plane-wave code supporting non-norm-conserving Vanderbilt-type US PP's,[15] the Vienna *ab initio* simulation package (VASP).[20,21] On the basis of the corresponding PAW-derived AE wave functions an implementation of the optical matrix elements is done for VASP. In the PAW approach AE wave functions $|\Psi_N\rangle$ are derived from pseudo (PS) wave functions $|\tilde{\Psi}_N\rangle$ by means of a linear transformation[18,19]

$$|\Psi_N\rangle = |\tilde{\Psi}_N\rangle + \sum_i \left(|\phi_i\rangle - |\tilde{\phi}_i\rangle\right)\langle \tilde{p}_i|\tilde{\Psi}_N\rangle. \tag{1}$$

The PS wave functions $|\tilde{\Psi}_N\rangle$ are the only variational quantities. The index $i$ is a shorthand for the atomic site $\mathbf{R}$, the angular momentum quantum numbers $l,m$, and the reference energies at which we construct the atomic partial waves $|\phi_i\rangle$ and $|\tilde{\phi}_i\rangle$. Both partial waves are obtained from a certain atomic reference configuration. As in the case of the PP method the AE partial waves $|\phi_i\rangle$ and the PS partial waves $|\tilde{\phi}_i\rangle$ are identical outside a core radius $r_c^i$ and match at $r_c^i$ being two times continuously differentiable. The PS partial waves are usually non-norm-conserving as in Vanderbilt's US PP scheme. Moreover, in contrast to PP schemes, they are even allowed to possess nodes. However, nodeless PS partial waves are usually preferred since they are much smoother. As in the US PP implementation a slightly modified Rappe-Rabe-Kaxiras-Joannopoulos pseudoization scheme[21,22] is used for the construction of the atomic PS partial waves. As in the case of US PP's the projectors $|\tilde{p}_i\rangle$ introduced in Eq. (1) are dual to the PS partial waves

$$\langle \tilde{p}_i|\tilde{\phi}_j\rangle = \delta_{ij}. \tag{2}$$

Also on the analogy of US PP's the PS wave functions fulfill generalized orthonormality constraints[19]

$$\langle \tilde{\Psi}_N|\hat{S}|\tilde{\Psi}_M\rangle = \delta_{NM} \tag{3}$$

with the overlap operator

$$\hat{S} = 1 + \sum_{i,j} |\tilde{p}_i\rangle\left(\langle\phi_i|\phi_j\rangle - \langle\tilde{\phi}_i|\tilde{\phi}_j\rangle\right)\langle\tilde{p}_j|. \tag{4}$$

The calculation of the matrix elements $\mathbf{p}_{NM} = \langle\Psi_N|\hat{\mathbf{p}}|\Psi_M\rangle$ of the momentum operator $\hat{\mathbf{p}}$ is straightforward using the ansatz Eq. (1) for the AE wave function $|\Psi_N\rangle$. One ends up with a formula that is formally identical to that given by Kageshima and Shiraishi:[13]

$$\mathbf{p}_{NM} = \langle\tilde{\Psi}_N|\hat{\mathbf{p}}|\tilde{\Psi}_M\rangle + \sum_{i,j}\langle\tilde{\Psi}_N|\tilde{p}_i\rangle\left(\langle\phi_i|\hat{\mathbf{p}}|\phi_j\rangle - \langle\tilde{\phi}_i|\hat{\mathbf{p}}|\tilde{\phi}_j\rangle\right)\langle\tilde{p}_j|\tilde{\Psi}_M\rangle. \tag{5}$$

In order to obtain this equation one has to use the completeness relation of the projector functions inside the augmentation sphere,[18]

$$\sum_i |\tilde{\phi}_i\rangle\langle\tilde{p}_i| = 1. \tag{6}$$

In all explicit numerical calculations Eq. (6) is fulfilled only approximately. However, the assumption that the projector basis is complete is one of the basic footings of the PAW method. It is analogous to the assumption made in the linearized muffin-tin method that the basis of augmentation functions inside the muffin-tin spheres is sufficiently complete.[23,24] The completeness of the projector basis can be controlled by the number of reference energies included in the projector basis. Sufficient completeness of the projector basis within the range of band energies of interest is always achieved by use of two reference energies, i.e., two projector functions per $lm$ channel. In our current implementation we limit the basis set to angular momentum quantum numbers $l \leq 2$, i.e., a proper augmentation of *s*, *p*, and *d* functions is taken into account. Higher $l$ quantum numbers are taken into account by a local PP, i.e., by pseudowave functions only.

The optical spectra resulting from DFT-LDA electronic structure calculations using the PAW approach are compared with those calculated within two other approaches. First, in order to demonstrate the AE aspect of the PAW method, we also present results based on the self-consistent full-potential linearized augmented plane-wave (FLAPW) method.[25,26] The code WIEN97 is used for explicit computations. Second, we compare the AE results with those of electronic structure calculations employing norm-conserving PP's.[8] Explicitly, the DFT-LDA code[27] FHI93CP is used. Two different methods of obtaining the optical matrix elements are possible. In the framework of the Coulomb gauge, $\mathbf{V}_{NM} = \langle\tilde{\Psi}_N|\hat{\mathbf{V}}|\tilde{\Psi}_M\rangle$ can be calculated using pseudowave functions $|\tilde{\Psi}\rangle$. We call this approach the transversal PP approach. However, one can also employ the longitudinal length gauge of the electromagnetic field where the optical transition operator is given by

$$\frac{\mathbf{q}}{q}\cdot\mathbf{p}_{NM} = (\varepsilon_N - \varepsilon_M)\frac{m}{\hbar}\lim_{\mathbf{q}\to 0}\left\langle \tilde{\Psi}_N\left|\frac{1}{q}e^{i\mathbf{q}\cdot\mathbf{x}}\right|\tilde{\Psi}_M\right\rangle \tag{7}$$

with the single-particle energies $\varepsilon_N$. We call this approximation the longitudinal pseudopotential (LPP) approach. Both gauges give supposedly identical results.[10] Therefore, we can restrict the computations to the use of one gauge. Since the explicit calculation of the full velocity operator matrix elements is quite cumbersome due to nonlocal contributions to the pseudopotentials, we avoid the Coulomb gauge. Thus, all PP results presented in this paper refer to the LPP approach. Details of the treatment can be found in Ref. 10. The three different electronic structure calculations have been carried out at the corresponding theoretical lattice constants, which are given in Table I. Additionally, Table I shows the cutoff energies for the plane-wave expansion for all materials and the different approaches. The tetrahedron method is applied to a Brillouin zone (BZ) integration employing 256 **k** points in the irreducible part of the BZ. The results are widely converged with respect to the number of conduction bands. For all calculations 100 conduction bands have been taken into account. All transition energies are taken in DFT-LDA quality. No quasiparticle corrections are considered. The calcula-

TABLE I. Lattice constants $a$ (in Å) and plane-wave cutoff energies $E_{cut}$ (in Ry) used within the three different methods FLAPW, PAW, and PP. The PAW values for GaAs and InSb given in parentheses refer to calculations treating the shallow $d$ core electrons explicitly as valence electrons. Within the FLAPW approach different cutoff energies are used for the different atoms of a compound.

| Method | Si | SiC | C | InSb | GaAs | AlP |
|---|---|---|---|---|---|---|
| | | | | $a$ | | |
| FLAPW | 5.41 | 4.33 | 3.53 | 6.49 | 5.61 | 5.44 |
| PAW | 5.41 | 4.33 | 3.54 | 6.34 (6.46) | 5.59 (5.61) | 5.44 |
| PP | 5.43 | 4.29 | 3.57 | 6.28 | 5.57 | 5.44 |
| | | | | $E_{cut}$ | | |
| FLAPW | 13 | 18/28 | 38 | 15/18 | 15/16 | 15/16 |
| PAW | 18 | 44 | 44 | 25 (45) | 25 (50) | 25 |
| PP | 15 | 34 | 42 | 15 | 15 | 15 |

tions are performed within the independent-particle approximation.[10] Hence, electron-hole interaction and local-field effects are not taken into account.

Moreover, in the PAW case we have performed two different calculations for the III-V compounds GaAs and InSb possessing shallow $d$ core electrons. The $d$ electrons can be frozen into the core or they can be explicitly treated as valence electrons. Whereas the first case reflects more the common situation in PP calculations, the latter reflects more closely the situation of full AE calculations. Therefore we considered both possibilities.

## III. RESULTS

First we compare results of the frozen-core PAW method with those obtained within the full all-electron FLAPW approach. In Figs. 1 and 2, linear optical absorption spectra and joint densities of states (JDOS's) are shown for the six cubic semiconductors Si, SiC, C, AlP, GaAs, and InSb. The agreement of the JDOS's is almost perfect for the materials with rather strongly localized core orbitals (Si, SiC, C, and AlP). Here, calculations performed within both approaches using the same lattice constant obviously lead to identical electronic structures. The same excellent agreement is found on comparing the optical absorption spectra for Si, SiC, C, and AlP. The line shapes and peak intensities are identical. The very narrow peaks in the Si and SiC PAW spectra, which do not occur in the FLAPW spectra, are due to a higher energy resolution. This means that the construction of AE wave functions using the frozen-core PAW method describes the true AE wave functions to a very high degree.

For the systems GaAs and InSb possessing more extended shallow core $d$ orbitals we find a reduced agreement (cf. Fig. 2) for the JDOS's as well as for the dielectric function. Differences in the optical spectra regard mostly the energetic positions of the main peaks as well as their intensities, whereas the overall line shapes are quite similar. As can be seen from the JDOS spectra in Fig. 2 these differences already appear in the electronic structures obtained within the two different approaches. For InSb they might be explained by the slightly different lattice constants (which is indicated by the variation of the PAW spectra with and without $d$ electrons). On the other hand, this explanation does not hold

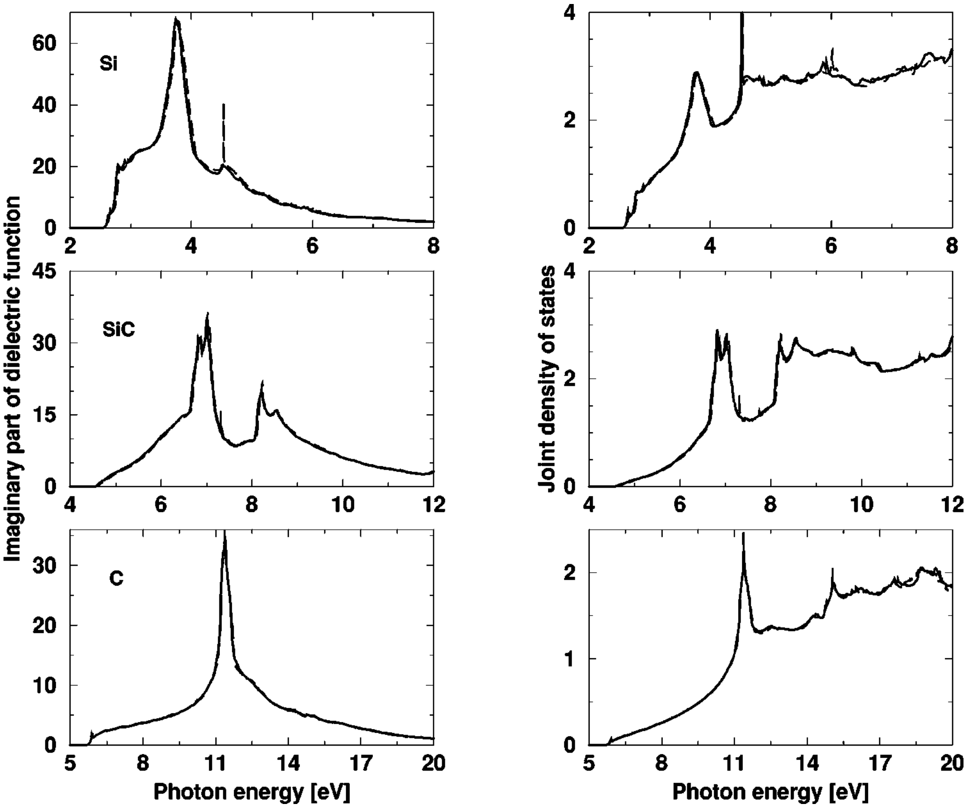

FIG. 1. Imaginary part of the dielectric function (left panel) and joint density of states (right panel) for the group-IV materials Si, SiC, and C. Solid line, FLAPW method; dashed line, PAW.

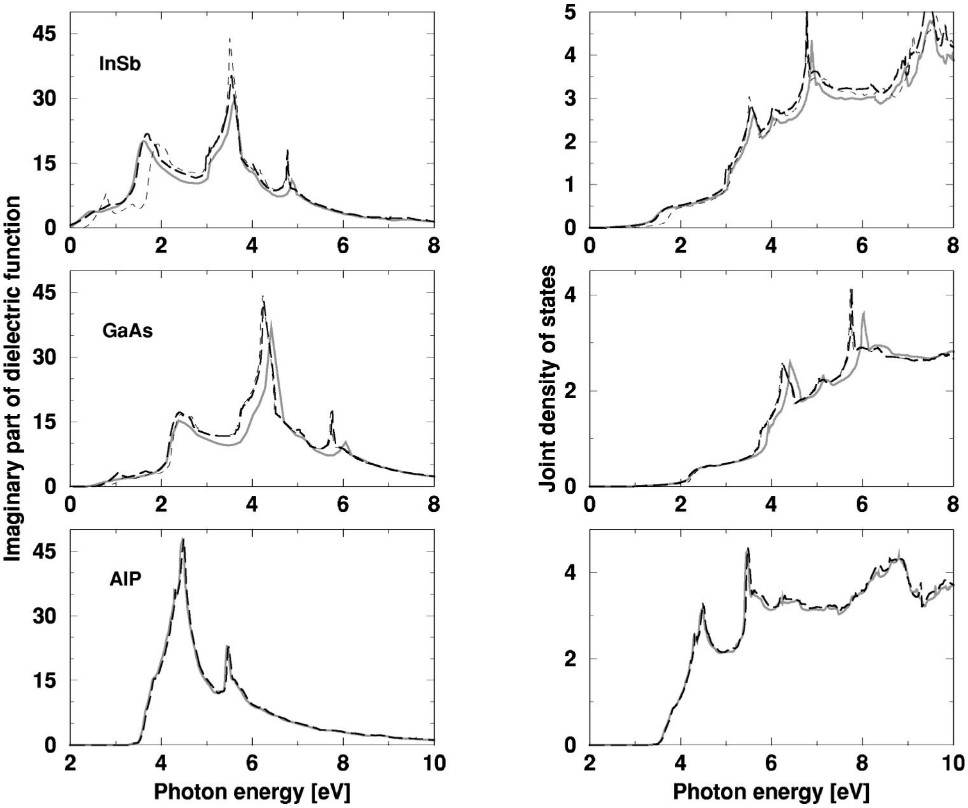

FIG. 2. Imaginary part of the dielectric function (left panel) and joint density of states (right panel) for the III-V compounds InSb, GaAs, and AlP. Solid line, FLAPW method; thin short-dashed line, PAW; thick long-dashed line, PAW including *d* core electrons.

for GaAs. An additional reason could be the frozen-core approximation employed in the PAW approach. The crucial point is that the worse energetic and spatial separation between core and valence states makes the frozen-core approximation more critical. Some of the problems associated with the frozen core may be solved by treating some of the shallow core states explicitly as valence states. However, it is often questionable which core states one has to consider. Inclusion, for example, of the *d* core states only might already be sufficient but in some cases even the corresponding *s* and *p* core states can still play a crucial role. Hence, inclusion of a limited subset of core states only may still provoke discrepancies with respect to a full AE approach such as the FLAPW method.

Taking the shallow *d* electrons into account explicitly as valence electrons (instead of putting them into the core) slightly improves the overall agreement between PAW and FLAPW optical spectra. Energetic positions and intensities of the main peaks within the two approaches agree better, particularly for the $E1$ peak and the low-energy tail of the spectra. This is observed for the dielectric function as well as for the joint density of states and seems to be reasonable, for the shallow *d* electrons are expected to influence mainly low-lying transitions. This also agrees with the effect that in the InSb case differences between the PAW results with and without *d* electrons become smaller and eventually vanish for increasing transition energies. Thus, even though the equilibrium lattice constants for the two calculations are somewhat different, the main effect on the optical spectra seems to be due to the treatment of the shallow *d* core states. In any case, slight discrepancies still remain with respect to a full AE approach such as the FLAPW method. This might indicate that even the explicit treatment of the shallow *d* states is not yet sufficient. However, we want to mention that, within the two approaches FLAPW and PAW, a lot of additional calculational parameters have to be considered as potential sources of error and have to be adjusted quite carefully to obtain well-converged results, especially for materials with rather extended core orbitals (like the shallow *d* states of GaAs and InSb). It cannot be excluded that an even better adjustment of those parameters might eventually lead to significantly better agreement between the two approaches. Besides the possible inclusion of even more core states in the PAW method, this may concern plane-wave cutoffs used (in particular in the FLAPW approach, cf. Table I), the choice of reference energies and pseudoization radii for the construction of the PAW partial waves, or the treatment of the shallow core states in the FLAPW methods, which may become rather critical if the extension of the core orbitals exceeds the muffin-tin radius. Therefore, further work has to be done in order to understand the remaining discrepancies in more detail.

The electronic dielectric constant $\varepsilon_\infty$ provides a good measure for the overall oscillator strengths, when it is calculated using the screening sum rules.[10] Corresponding results are given in Table II. There, in the cases of GaAs and InSb note to the PAW values of the dielectric constant given in parentheses, which correspond to calculations that explicitly include the shallow *d* core states as valence states. These calculations should reflect a true AE calculation much more closely than calculations freezing the *d* electrons into the core. The main effect of the *d* electrons is to change the lattice constant slightly, resulting in a decrease of the fundamental gap. In the case of InSb one even ends up with semi-

TABLE II. Dielectric constant $\varepsilon_\infty$ calculated within the three different methods FLAPW, PAW, and PP. The PAW values for GaAs and InSb given in parentheses refer to calculations treating the shallow *d* core electrons explicitly as valence electrons.

| Method | Si | SiC | C | InSb | GaAs | AlP |
|---|---|---|---|---|---|---|
| FLAPW | 13.6 | 7.2 | 5.9 | 20.0 | 12.7 | 9.0 |
| PAW | 13.8 | 7.1 | 5.9 | 17.3 (21.0) | 13.5 (14.4) | 8.9 |
| PP | 13.5 | 7.4 | 6.2 | 13.9 | 11.9 | 8.7 |

metallic behavior. The decrease of the fundamental gap upon inclusion of the *d* electrons mainly influences the low-energy tail of the PAW spectra in Fig. 2. This change of the low-energy tail causes most of the observed changes of the dielectric constants. In addition, for InSb the strength of the main peak is also somewhat reduced whereas in the case of GaAs the changes in the spectra are almost negligible for transition energies larger than 3 eV (which the change in lattice constant is). The dielectric constants within both approaches show very good overall agreement, particularly for the less critical systems C, SiC, Si, and AlP. Even for InSb the agreement is rather good if we compare with the PAW result including the *d* electrons as valence electrons and if we take into account that the semimetallic character of InSb in the AE DFT-LDA treatment gives rise to rather unphysical and numerically critical low-energy tails in the spectra. Only for GaAs does the observed discrepancy become slightly worse after inclusion of the *d* electrons. The difference is traced back to the lower peak intensities in the FLAPW spectra for GaAs, leading to a smaller dielectric constant compared to the PAW method. Nevertheless, since the agreement is still reasonable, we conclude that our AE approach to the wave functions in the framework of the PAW method gives very reliable results. Linear optical properties of the valence electrons using PAW wave functions can therefore be considered as representing true AE spectra.

In Figs. 3 and 4 we compare the PAW-derived AE spectra described with spectra calculated with norm-conserving pseudo wave functions and in longitudinal gauge of the electromagnetic field for all six semiconductors. Both the imaginary part of the dielectric function and the JDOS are plotted. Again, the JDOS shows the very good agreement of the electronic structures of the six semiconductors considered calculated within the two different approaches. The small differences in the JDOS are mainly a consequence of the different theoretical lattice constants due to the different calculational schemes used. The absorption spectra also show very good agreement for almost all materials. Apart from significant differences in the low-energy region of the spectra for GaAs and InSb, the line shapes of all spectra are rather independent of the electronic structure method used in the calculation. We find very small differences in the peak intensities due to slightly different transition matrix elements. The stronger difference for the peak at 4.5 eV in the Si spectrum is again due to different energy resolutions of the spectra. The small deviations in the peak positions can be explained by the small differences in the lattice constants. The observed overall agreement in the frequency dependence of the dielectric functions calculated within the PP and PAW methods indicates that the exact shape of the wave functions in the core regions does not play an important role in the linear optical

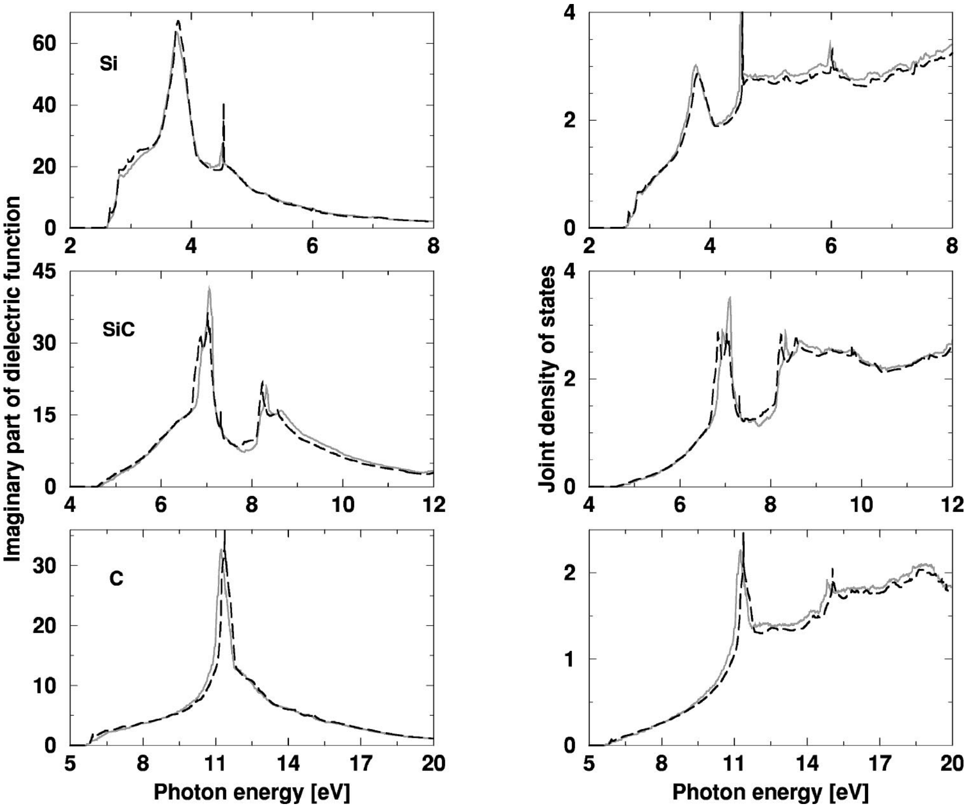

FIG. 3. Imaginary part of the dielectric function (left panel) and joint density of states (right panel) for the group-IV materials Si, SiC, and C. Solid line, PP approach; dashed line, PAW method.

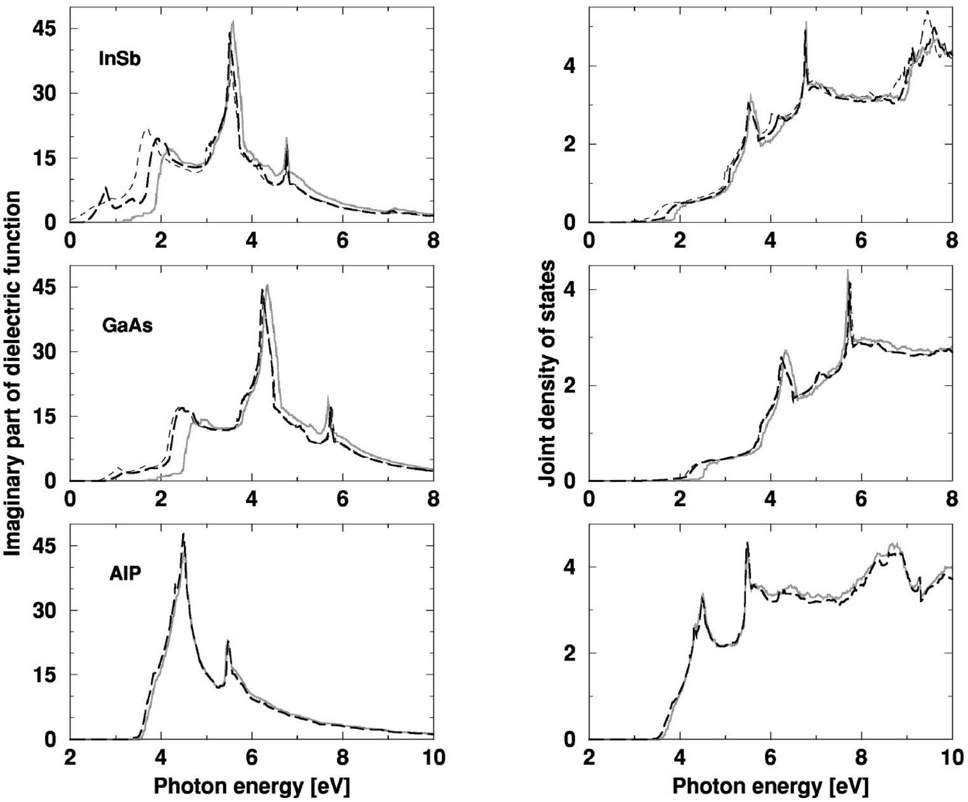

FIG. 4. Imaginary part of the dielectric function (left panel) and joint density of states (right panel) for the III-V compounds InSb, GaAs, and AlP. Solid line, PP approach; thick long-dashed line, PAW; thin short-dashed line, PAW including *d* core electrons.

properties for materials with rather localized core orbitals such as Si, SiC, C, and AlP.

The situation is different for the III-V compounds GaAs and InSb, which include elements with shallow *d* core states. For this class of materials, the PP approach should generally suffer more seriously from the improper nodal structure of the valence wave functions in the core region than for materials possessing very localized core states that are well separated from the valence states. Due to the stronger core-valence overlap in GaAs and InSb the PS wave functions already deviate strongly from the AE wave functions in the region where they not only still do overlap but also interact significantly with the shallow core orbitals. The expected consequence is an insufficient description of the core-valence interactions and, hence, of the valence states themselves. Even treatment of the shallow core states as valence states does not improve this situation in a satisfying manner. In addition to this general problem, which already occurs in total-energy calculations, i.e., the calculation of equilibrium lattice constants, cohesive energies, or single-particle band structures, the calculation of optical matrix elements also suffers from another problem. The error introduced by the improper description of the nodal structure of the wave functions is most probably increasing with increasing volume fraction of the pseudocore region where the PS wave functions deviate significantly from the AE ones. Since one is forced to pseudoize the AE wave functions outside the outermost node this volume fraction is directly determined by the position of this node. However, this position is approximately determined by the position of the maximum of the energetically highest core state and hence is related to the extension of this core state. This is a general rule, which reflects the orthonormality constraints of the atomic wave functions. Due to the much weaker localization of the shallow core states in GaAs and InSb, one would expect that the volume fraction of the improperly described pseudocore region becomes significantly larger than for systems with very localized core states as C, SiC, Si, and AlP. Consequently, the more extended core region in the case of GaAs and InSb should provoke larger errors compared to the other materials.

The main difference in the optical spectra concerns the underestimation of the $E_0$ and $E_1$ transitions (for nomenclature of the optical transitions see, e.g., Ref. 28) using the PP method. This discrepancy already occurs, to a smaller extent, in the JDOS spectra. However, we observe as well an effect of underestimating the matrix elements of the lowest optical transitions close to the BZ center. As we demonstrate in Table III, the matrix elements in the PAW approach are clearly larger than the PP ones for the low-energy transitions $E_0$, whereas for energetically higher transitions both approaches lead to nearly identical matrix elements. Moreover, for GaAs Kageshima and Shiraishi[13] calculated matrix elements of $0.30(E_0)$, $0.34(E_1)$, and $0.23(E_2)$ $(\hbar/a_B)^2$ which agree well with the PAW values in Table III, confirming the discrepancies found with respect to the PP results. Hence, the differences in the low-energy regions of the spectra are obviously related to the different quality of the treatment of the core part of the valence wave functions. This is also supported by the fact that treating the shallow *d* states explicitly as valence states leads to even stronger differences between the PAW and PP results (cf. Fig. 4) but can by no means be considered the only reason for the discrepancies observed.

Table II gives a comparison of the electronic dielectric constant $\varepsilon_\infty$ for the PAW method and the PP approach as

TABLE III. Square of momentum matrix elements in atomic units $(\hbar/a_B)^2$ (first value) and DFT-LDA transition energy in eV (second value) for important optical transitions in the materials under consideration. The electronic structure calculation method is characterized by the wave functions used. The PAW values for GaAs and InSb in parentheses refer to calculations including the *d* core electrons as valence electrons.

| Method | $E_0$ | | $E_1$ | | $E_0'$ | | $E_2$ | | $E_1'$ | |
|---|---|---|---|---|---|---|---|---|---|---|
| Si | | | | | | | | | | |
| PAW | 0.14 | 2.54 | 0.35 | 2.68 | 0.32 | 3.31 | 0.26 | 3.50 | 0.21 | 4.53 |
| PW | 0.14 | 2.54 | 0.33 | 2.68 | 0.28 | 3.29 | 0.25 | 3.46 | 0.21 | 4.49 |
| SiC | | | | | | | | | | |
| PAW | 0.27 | 6.54 | 0.40 | 6.65 | 0.21 | 7.33 | 0.31 | 4.57 | 0.30 | 8.30 |
| PW | 0.27 | 6.80 | 0.37 | 6.75 | 0.21 | 7.48 | 0.28 | 4.46 | 0.30 | 8.28 |
| C | | | | | | | | | | |
| PAW | 0.29 | 5.64 | 0.42 | 11.36 | 0.27 | 14.26 | 0.57 | 11.28 | 0.52 | 12.31 |
| PW | 0.27 | 5.53 | 0.39 | 11.23 | 0.26 | 13.93 | 0.54 | 11.12 | 0.51 | 12.08 |
| InSb | | | | | | | | | | |
| PAW | 0.31 | 0.24 | 0.32 | 1.68 | 0.14 | 3.09 | 0.21 | 3.46 | 0.21 | 4.84 |
| | (0.28) | (-0.35) | (0.30) | (1.46) | (0.16) | (2.97) | (0.22) | (3.56) | (0.23) | (4.86) |
| PW | 0.12 | 0.71 | 0.28 | 1.86 | 0.16 | 3.15 | 0.23 | 3.45 | 0.24 | 4.83 |
| GaAs | | | | | | | | | | |
| PAW | 0.33 | 0.66 | 0.37 | 2.18 | 0.17 | 3.79 | 0.25 | 4.05 | 0.25 | 5.82 |
| | (0.32) | (0.48) | (0.36) | (2.13) | (0.18) | (3.75) | (0.26) | (4.11) | (0.26) | (5.85) |
| PW | 0.17 | 1.26 | 0.33 | 2.46 | 0.17 | 3.80 | 0.26 | 4.05 | 0.26 | 5.75 |
| AlP | | | | | | | | | | |
| PAW | 0.28 | 3.19 | 0.32 | 3.49 | 0.15 | 4.51 | 0.21 | 3.60 | 0.21 | 5.54 |
| PW | 0.23 | 3.26 | 0.28 | 3.54 | 0.14 | 4.54 | 0.19 | 3.59 | 0.20 | 5.53 |

well. The relationships of the values calculated within the PAW and PP methods confirm the above discussion of the absorption spectra. We observe again good agreement of the PAW and PP results for Si, SiC, C, and AlP. The PAW values for GaAs and InSb are underestimated by the PP method, which reflects the underestimation of the low-energy tail of the spectra. However, we find rather good overall agreement of the results obtained using different methods.

## IV. SUMMARY

The dielectric functions of the group-IV and III-V semiconductors Si, SiC, C, InSb, GaAs, and AlP have been calculated by means of the (frozen-core) all-electron projector-augmented wave method, which possesses a close relationship to Vanderbilt's non-norm-conserving US PP. By using the PAW method it becomes possible to calculate physical properties involving wave functions very accurately, despite the fact that the underlying variational quantities remain non-norm-conserving pseudowave functions, which are just augmented in a different way.

Comparing our results with those obtained within the FLAPW method, we found that the PAW treatment of the optical transition matrix elements reproduces linear optical properties from a full all-electron method very well for materials with rather localized core electrons. For GaAs and InSb, possessing extended shallow *d* core orbitals, the agreement found is reduced but still quite reasonable. This holds for spectra as well as for dielectric constants. The differences occurring may be due to the fact that a sufficiently well converged description of particularly the extended *d* core orbitals is a difficult task to achieve within the different numerical approaches. However, the PAW approach can reasonably be considered a quasi-all-electron method.

For all materials under consideration the absorption spectra have also been compared with spectra calculated by means of a common pseudopotential-plane-wave method. For systems with more localized core states such as C, Si, SiC, and AlP, we have shown that the different treatment of the wave functions in the core region has a minor influence on the linear optical properties. Thus, for these materials a standard PP calculation using norm-conserving PP's can be considered sufficient for linear optics. For systems with more extended shallow *d* core orbitals like GaAs and InSb, the PAW method improves in particular the underestimation of the $E_0$ and $E_1$ peaks within a PP treatment using norm-conserving PPs.

## ACKNOWLEDGMENTS

We thank O. Pulci, J. E. Sipe, A. Shkrebtii, and U. Birkenheuer for useful discussions. This work was financially supported by the Deutsche Forschungsgemeinschaft (SFB 196, Project Nos. A8 and Be 1346/10-1).

[*] Present address: Department of Physics, University of Toronto, 60 St George Street, Toronto, ON, Canada M5S 1A7.

[1] F. Bechstedt, K. Tenelsen, B. Adolph, and R. Del Sole, Phys. Rev. Lett. **78**, 1528 (1997).
[2] S. Albrecht, L. Reining, R. Del Sole, and G. Onida, Phys. Rev. Lett. **80**, 5410 (1998).
[3] L.X. Benedict, E.L. Shirley, and R.B. Bohn, Phys. Rev. Lett. **80**, 4514 (1998); Phys. Rev. B **57**, R9385 (1998).
[4] M. Rohlfing and S.G. Louie, Phys. Rev. Lett. **81**, 2312 (1998).
[5] L.X. Benedict and E.L. Shirley, Phys. Rev. B **59**, 5441 (1999).
[6] P. Hohenberg and W. Kohn, Phys. Rev. **136**, B864 (1964).
[7] W. Kohn and L.J. Sham, Phys. Rev. **140**, A1133 (1965).
[8] G.B. Bachelet, D.R. Hamann, and M. Schlüter, Phys. Rev. B **26**, 4199 (1982).
[9] A.F. Starace, Phys. Rev. A **3**, 1242 (1971).
[10] B. Adolph, V.I. Gavrilenko, K. Tenelsen, F. Bechstedt, and R. Del Sole, Phys. Rev. B **53**, 9797 (1996).
[11] M.S. Hybertsen and S.G. Louie, Phys. Rev. B **35**, 5585 (1987).
[12] A.J. Read and R.J. Needs, Phys. Rev. B **44**, 13 071 (1991).
[13] H. Kageshima and K. Shiraishi, Phys. Rev. B **56**, 14 985 (1997).
[14] R. Asahi, W. Mannstadt, and A.J. Freeman, Phys. Rev. B **59**, 7486 (1999).
[15] D. Vanderbilt, Phys. Rev. B **41**, 7892 (1990).
[16] J. Furthmüller, P. Käckell, F. Bechstedt, and G. Kresse, Phys. Rev. B **61**, 4576 (2000).
[17] A. Zywietz, J. Furthmüller, and F. Bechstedt, Phys. Rev. B **59**, 15 166 (1999).
[18] P.E. Blöchl, Phys. Rev. B **50**, 17 953 (1994).
[19] G. Kresse and D. Joubert, Phys. Rev. B **59**, 1758 (1999).
[20] G. Kresse and J. Hafner, Phys. Rev. B **47**, R558 (1993); J. Phys.: Condens. Matter **6**, 8245 (1994).
[21] G. Kresse and J. Furthmüller, Comput. Mater. Sci. **6**, 15 (1996); Phys. Rev. B **54**, 11 169 (1996).
[22] A.M. Rappe, K.M. Rabe, E. Kaxiras, and J.D. Joannopoulos, Phys. Rev. B **41**, 1227 (1990).
[23] O.K. Andersen, Phys. Rev. B **12**, 3060 (1975).
[24] H. L. Skriver, *The LMTO Method* (Springer-Verlag, Berlin, 1984).
[25] P. Blaha, K. Schwarz, P. Sorantin, and S.B. Trickey, Comput. Phys. Commun. **59**, 399 (1990).
[26] K. Schwarz and P. Blaha, Lect. Notes Chem. **67**, 139 (1996).
[27] R. Stumpf and M. Scheffler, Comput. Phys. Commun. **79**, 447 (1994).
[28] P. Y. Yu and M. Cardona, *Fundamentals of Semiconductors* (Springer, Berlin, 1996).